

Viewpoint Paper

Microstructural stability during cyclic loading of multilayer copper/copper samples with nanoscale twinning

C.J. Shute,^a B.D. Myers,^a S. Xie,^a T.W. Barbee Jr.,^b A.M. Hodge^c and J.R. Weertman^{a,*}

^aNorthwestern University, Evanston, IL 60208, USA

^bLawrence Livermore National Laboratory, Livermore, CA 94550, USA

^cUniversity of Southern California, Los Angeles, CA 90089-1453, USA

Received 1 October 2008; revised 21 November 2008; accepted 24 November 2008

Available online 30 December 2008

Abstract—The response to cyclic deformation has been studied for Cu/Cu multilayer material consisting of columns of closely spaced, parallel nanotwins. The fatigue life under stress-controlled cycling is greatly improved over that of coarse-grained Cu. Nanotwinning provides significant strengthening, which is unchanged by fatigue or severe compression. Observations by focused ion beam microscopy showed that the microstructure is quite stable under deformation. Localized deformation from indentation produced shear bands and apparently some loss of nanotwinned area but no decrease in hardness.

© 2008 Acta Materialia Inc. Published by Elsevier Ltd. All rights reserved.

Keywords: Nanostructured materials; Twinning; Copper; Fatigue test; FIB

Introduction

The early enthusiasm generated by the confirmation of significant Hall–Petch strengthening [1,2] in metals with grain size in the nanocrystalline range (<~100 nm) was quickly tempered by observations of the brittle nature of this class of materials, their frequent microstructural instability under stress, and their lower electrical conductivity [3–5]. In contrast, extensively nanotwinned Cu has been shown not only to be stronger than coarse-grained copper, but also to be thermally stable, reasonably ductile and having good electrical conductivity [4,6–9]. Hodge and colleagues [10,11] have carried out extensive characterization of the behavior under tensile deformation of high-purity Cu consisting of parallel twins with twin interface spacing in the range of a few tens of nanometers. In the present study, we examine the results of time-dependent stress, compression and highly localized stress on this material.

Experimental details

Nanotwinned Cu was produced by magnetron sputtering multiple layers of ultrahigh-purity (99.999%) Cu

on (100) Si wafers. The results are columns, perpendicular to the growth direction, of aligned twins separated by (111) interfaces. The spacing between the parallel twin interfaces can be varied by adjusting the sputtering time spent on each of the two Cu targets. (Details of the synthesis process are given in Refs. [10,11]). The copper samples used in the present study all came from one deposition. The thickness of the sputtered copper, 178 μm , was sufficient to allow it to be carefully removed from the Si wafer and handled as a free-standing foil.

Strength estimates were made from measurements of the Vickers hardness on the As-deposited material and after compression testing. The hardness measurements were made with a 100 g load and dwell time of 5 s.

Dog-bone samples for tension–tension fatigue testing were cut from the wafer, initially using a template, steel blade and carbide deburring tool. This method left edge defects, and so a change was made to cutting by electro-discharge machining (EDM). Any rough edges or scratches visible under an optical microscope were polished with a series of diamond suspensions and alumina slurries to a submicrometer finish. The gage length for all tension–tension fatigue samples was 6.7 mm and the width was ~3 mm. The thickness of the samples was about 170 μm . Samples were fatigued in tension–tension in an MTS 810 servohydraulic testing machine. A special grip which facilitated alignment of these

* Corresponding author. E-mail: jrweertman@northwestern.edu

samples was used to prevent bending during loading of the samples. The first test, of a sample cycled with a maximum stress of 372 MPa, was carried out with a frequency of 1 Hz, but a frequency of 10 Hz was used for all subsequent tension–tension tests. All fatigue tests were conducted with a stress ratio ($\sigma_{\min}/\sigma_{\max}$) of 0.1.

For compression testing, 3 mm discs were cut from the Cu/Cu wafer by EDM. The edges and flat surfaces of the discs were polished to a 1 μm finish. Samples were placed between two polished WC platens which were lubricated with Dry Moly[®] and 3-in-One[™] oil. Three samples were compressed at a rate of 10^{-3} s^{-1} to engineering stresses of 863, 1800 and 3840 MPa. These compression tests were performed on a Sintech 20/G servoelectric load frame. In addition, one of the Cu/Cu foils was fatigued on the MTS 810 servohydraulic machine between -56 and -560 MPa for 5000 cycles at 10 Hz.

The effect of a highly localized stress on the internal structure of the Cu/Cu material was examined by indenting a sample with a Vickers microhardness indenter applied at 2000 g for 5 s.

To observe the effects on the internal structure caused by the various modes of deformation imposed on the nanotwinned Cu, transverse cuts were milled out with a focused ion beam (FIB) using a FEI Helios Nanolab 600 instrument. The microstructure of the cut region was imaged using ion channeling contrast with a very low current (30 kV, 9.7 pA) ion beam and an Everhart–Thornley (E-T) detector. Dislocation activity was studied from transverse electron-transparent foils made and thinned by the FIB. The transmission electron microscopy (TEM) foils were examined in a JEOL 2100 FasTEM operating at 200 kV.

Results

The dependence of fatigue life N_f on the cyclic stress range ($\sigma_{\max}-\sigma_{\min}$) is plotted in Figure 1. The two samples fatigued at the highest stress levels showed some necking; failure occurred in the gage length. For all other failed samples the failure took place close to one of the grip ends, possibly due to sample alignment diffi-

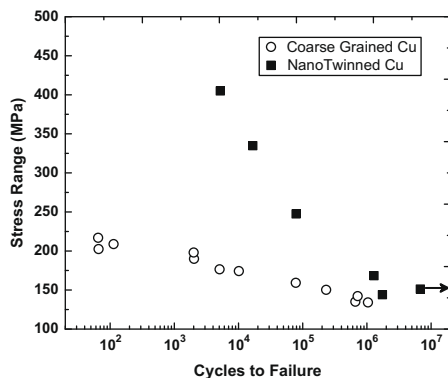


Figure 1. Plot of tensile stress range vs. cycles to failure for the Cu/Cu nanotwinned samples. Also shown is a similar plot for coarse-grained Cu (from Ref. [12]).

culties or the complex stress state in this region. Also shown in Figure 1 is an analogous S–N plot for high-purity coarse-grained Cu [12]. It can be seen that the decrease in the microstructural length scale provided by the nanotwins greatly improves fatigue life. While this difference in fatigue life is obvious in the high stress range part of the curve, even at the lower stresses the difference can be seen to be considerable when the numbers of cycles to failure at a given stress range are compared for the two microstructures. For example, at a stress range of 150 MPa, Figure 1 predicts that the nanotwinned Cu should last about 10 million cycles longer than the coarse-grained Cu.

The As-deposited Cu/Cu multilayer disc had a mirror-like surface on the face that was in contact with the substrate during deposition and a dull surface on the other side. The dull surface could easily be polished to a mirror finish with 3 μm diamond paste followed by one of 1 μm . Hardness measurements on the two sides revealed a considerable difference. The Vickers hardness on the substrate side was 1.1 GPa while that on the other side was 1.9 GPa. The corresponding penetration depths (1/7 indenter diameter) were 4.2 and 5.7 μm with the same load of 100 g and 5 s dwell time. Both surfaces were further polished and their hardness remeasured. A removal of approximately 15 μm from the harder side did not change its hardness value, whereas polishing off ~ 15 to 20 μm from the substrate side increased the hardness from 1.1 to 1.8 GPa.

Transverse cuts were milled out close to the two surfaces by a FIB. The internal structure in these regions was imaged using ion channeling contrast with a very low current ion beam (30 kV, 9.7 pA). Figure 2a and b shows the ion beam images for the soft and hard sides of the As-deposited Cu/Cu foil. As can be seen from the images, the structure changes dramatically from non-columnar near the soft side (Fig. 2a) to highly oriented nanotwinned columns on the hard side with twin interfaces perpendicular to the growth direction (Fig. 2b). For all FIB images, the top of the image is at, or very close to, the sample surface; the bottom of the image is in the sample interior.

The FIB images for the hard side of an As-deposited sample (Fig. 2b) show two basic types of columns. A few columns contain a number of approximately equiaxed

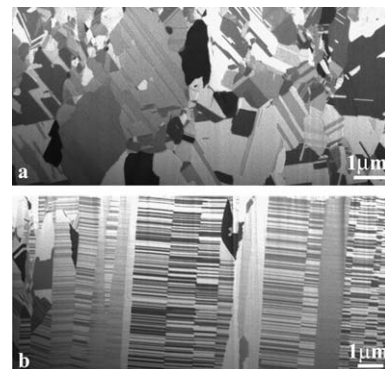


Figure 2. FIB images showing the transverse microstructure of (a) the soft (substrate) side; (b) the hard side (free surface during deposition) of an As-deposited Cu/Cu multilayer sample.

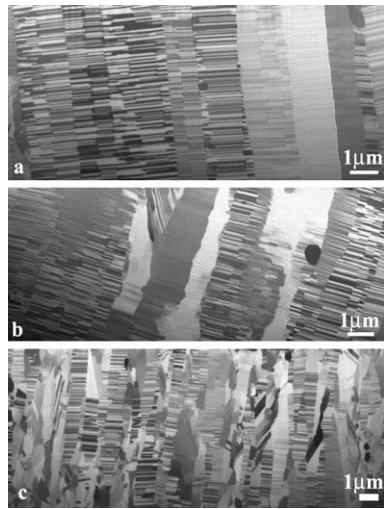


Figure 3. FIB images showing the transverse microstructure taken from the harder surface of Cu/Cu multilayer samples subjected to tension–tension fatigue with a maximum stress of (a) 187 MPa; (b) 372 MPa; (c) 450 MPa. All images were taken close to the fracture site. The tensile stress axis was parallel to the twin interfaces.

grains, but most columns are 100% twinned with straight twin interface boundaries normal to the growth direction. The boundaries between columns also are straight. Some of the twinned columns show some interlacing or fragmentation of the column boundaries. A few columns here and in subsequent FIB images appear blank or only faintly show the underlying microstructure. These regions were probably not oriented as well as other areas with respect to the ion beam for good channeling contrast or may have ion-induced surface amorphization. Figure 2a shows that the substrate or soft side of the sample consists of non-columnar grains with a wide range of sizes less than a micrometer to several micrometers in one or more directions.

FIB images (Fig. 3a–c) were prepared from transverse cuts of samples cycled in tension–tension fatigue at maximum stresses of 187, 372 and 450 MPa. All cuts were made near the fracture site from the hard, highly twinned surface of the samples. The applied stress acted parallel to the twin interfaces. As can be seen from a comparison of these images with Figure 2b, the twinned microstructure is quite stable, even under the highest fatigue stress. There is little change or only a slight decrease in the spacing between the twin interfaces. However, there is some fragmentation of the columns and conversions of twinned columns into irregular columns of equiaxed grains, especially evident in the case of the sample fatigued at the highest stress level of

450 MPa. The straight columns of the As-deposited material give way to irregularly shaped, elongated regions with the twin interfaces approximately perpendicular to their long axes.

A summary of the results of the compression tests and post-compression hardness measurements is given in Table 1. The surfaces of samples Comp2 and Comp3, which were compressed to engineering stresses of 1800 and 3840 MPa, respectively, were broken into a mosaic-type structure with flat regions completely surrounded by cracks. These flat regions were chosen for the hardness measurements and for subsequent transverse ion beam imaging. The hardness values measured on both sides of samples Comp1 and 2 after compression were unchanged from those of the As-deposited material. Hardness measurements could not be made on the most highly stressed sample, Comp3, because it was dome-shaped after compression as a result of residual stresses. Hardness was also measured on sample Comp4, which had been cycled between compressive stresses of -56 and -560 MPa for 5000 cycles. Note that the stress axis in the Comp samples acted perpendicular to the twin interfaces rather than parallel to them, as in the case of tension–tension fatigue.

Ion beam images of samples Comp2 and Comp4 after testing are shown in Figure 4a and b. In the case of the sample fatigued in compression for 5000 cycles (Comp4, Fig. 4a), the column boundaries remained smooth but some columns are split as the twin interfaces came out of registry. This splitting is also seen in the highly compressed Comp2 sample (Fig. 4b). Here the column boundaries have become quite irregular.

To examine the effect on the microstructure of a complex stress, an indentation was made on the hard surface of an As-deposited sample by a Vickers microhardness indenter under a load of 2000 g for 5 s. As before, the hardness value was found to be 1.8 GPa. The diameter of the indentation at the surface was 144 μm , giving a penetration depth of 21 μm . The indented surface was then polished to bring the tip of the indented region within easy range for a transverse FIB cut and viewing. Figure 4c shows an ion beam image near the bottom of the indented region. The dark band across the top of the cut is a layer of platinum that was deposited to protect the sample surface and minimize curtaining effects during ion milling. Figure 4c is centered on a region a little to one side of the line followed by the indenter tip (indicated by an arrow). Changes to the initially highly twinned columnar microstructure are quite evident. A shear band runs from the indented tip region roughly 60° with respect to the vertical line of the indenter. A vertical column of equiaxed grains has formed directly

Table 1. Summary of compression tests.

Sample	Test (MPa)	Diameter change (%)	Hardness (GPa) soft side ^b	Hardness (GPa) hard side ^b
As-Is	–	–	1.1	1.9
Comp1	Compressed to 863	2	1.1	1.7
Comp2	Compressed to 1800	13	1.2	1.8
Comp3 ^a	Compressed to 3840	35 ^a	–	–
Comp4	Fatigued, 5000 cycles (-56 to -560)		1.1	1.8

^a Sample was dome-shaped after testing.

^b Post-testing hardness values.

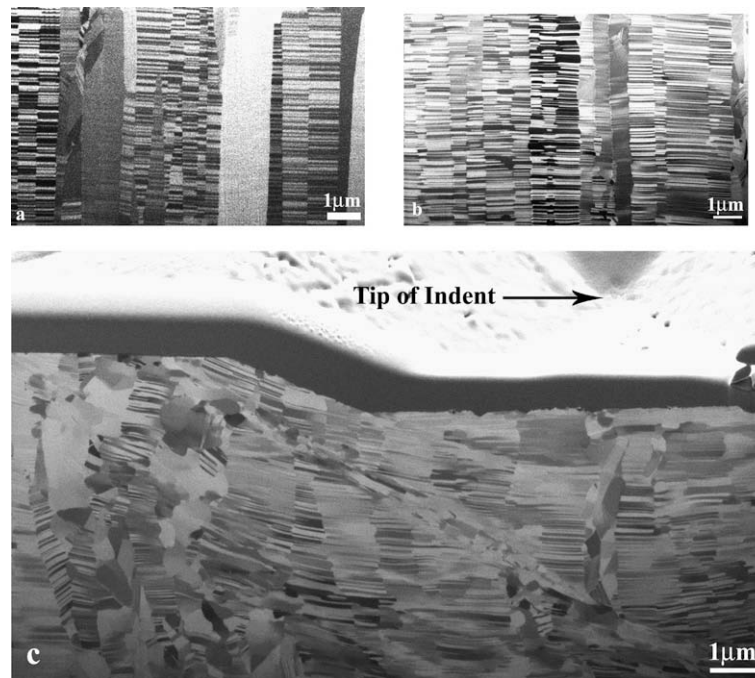


Figure 4. FIB image of a transverse cut made on the hard side of a Cu/Cu multilayer sample (a) after fatiguing through 5000 cycles between -56 and -560 MPa (Comp4); (b) after compressive loading to 1800 MPa (Comp2); (c) near the bottom of an indent. The arrow shows the position of the indenter. In (a) and (b) the stress is perpendicular to the twin interfaces.

under the indenter tip. A large region is visible in the left-hand portion of Figure 4c that clearly consists of equiaxed grains. The twinning has become indistinct in some regions, but there is insufficient evidence at present to determine the cause of this change. The process by which some regions of the material lose their nanotwinned structure under deformation is important and merits further study.

Transmission and high-resolution electron microscopy observations were made of thin foils prepared by FIB (pictures not shown because of space limitations). Dislocations are seen in the interiors of twins in deformed samples that extend from a twin boundary to the adjacent boundary, but do not travel into the next twin. There is an indication of high stresses in the vicinity of the twin interfaces. Some interfaces bend. There are incoherent regions along them, a few nanometers in height. Evidence of detwinning is seen in the sample subjected to indentation.

Discussion

FIB microscopy has proven to be an invaluable tool for examining the effect of deformation on the transverse microstructure of the Cu/Cu multilayer samples. Sufficient areas can be scrutinized to determine variations in internal structure: twinned columns, other columns with equiaxed grains, shear bands. The technique allows for sectioning at well-specified regions, such as through an indentation.

The Cu/Cu multilayer samples present several length scales. The spacing between twin interfaces in the heavily twinned columns is some tens of nanometers. In the case of columns that are not closely twinned but instead con-

tain equiaxed grains, the average size of these grains is in the ultrafine grain (submicrometer) range. The width of the columns, and thus the width of the twin interfaces, is about a micrometer or slightly less. Another length scale is the column length. This last length has not been determined in the current study but it is obviously much larger than any of the other length scales since most of the columns were at least as long as the depth of the FIB sections that were cut for imaging.

Several investigators have studied the influence of the spacing between twin interfaces on strength, similar to the strengthening effect of ordinary grain boundaries [13,14]. Twinning also has been used to explain increased ductility in Cu with nano-length-scale microstructure. The width of the twin interface boundaries may be an important parameter for controlling ductility [6,15].

The significant strengthening provided by the nanotwinned microstructure of the Cu/Cu samples is demonstrated by comparing the hardness of the substrate surface and the surface that remained free during deposition. These values were 1.1 and 1.8 GPa, respectively, close to a 50% difference. The transverse FIB images of Figure 2a and b show roughly equiaxed grains of a size $1\ \mu\text{m}$ or greater on the substrate side, and on the harder side closely spaced nanotwins, arranged in columns, with the twin interfaces parallel to the sample surface. Further evidence of the strengthening offered by the nanotwinned microstructure is the increase in hardness of the substrate side up to that of the harder surface once the layer of equiaxed grains is polished away.

The fatigue behavior of the nanotwinned Cu/Cu multilayer materials is considerably improved over that of coarse-grained Cu. This is to be expected in stress-controlled cycling, where strength is important. Tests run

in strain-control are not likely to be so favorable for the multilayer material, since ductility rather than strength is needed here [16].

The TEM and high-resolution electron microscopy (HREM) pictures show that the twin interface boundaries are effective in stopping dislocations and preventing them from continuing through the material, as was previously observed by Dao et al. [6]. In the samples subjected to tension–tension or compression–compression fatigue or simple compression, the applied stress was either parallel or perpendicular to the twin interfaces. In the case of indentation the stress state was more complex with shear components. A shear band formed at roughly 60° with respect to the vertical line of the indenter (Fig. 4c). Appreciable areas have changed from nanotwinned regions to a roughly equiaxed microstructure in the indented sample. Cycling with a shear component parallel to the twin interface should be of interest.

The nanotwinned microstructure not only has superior strength, it also provides stability, unlike equiaxed nanocrystalline Cu that quickly undergoes large grain growth under stress [5,17]. The hardness of the Cu/Cu material undergoes no noticeable decrease even under the most severe deformation used in this investigation. As Figures 3 and 4 show, the columns may become a little wobbly and the nanotwins of a few columns be replaced by equiaxed grains but the spacing of the twin interfaces remains the same or even decreases slightly.

Summary and Conclusions

A study has been carried out on the effect of cyclic deformation on Cu/Cu multilayer material consisting of columns of closely spaced, parallel nanotwins.

- High purity nanotwinned Cu is much more stable under deformation than equiaxed nanocrystalline Cu.
- The fatigue life of the nanotwinned Cu under stress-controlled tension–tension cycling is much improved over that of coarse-grained Cu.
- It was found that the nanotwinned microstructure is ~50% stronger than a structure made up of micrometer-sized equiaxed grains.
- Although transverse images observed by FIB microscopy showed that fatigue and severe compression produce changes to the columnar structure, including conversion of some columns from nanotwins to equiaxed grains, no change in hardness was detected. The nanotwinned structure is quite stable under deformation.

- Highly localized deformation from a microhardness indenter produced shear bands and changed some previously nanotwinned regions to roughly equiaxed microstructures, although not enough to affect the hardness.
- TEM and HREM pictures from FIB-produced foils from transverse cuts showed dislocations traversing twins but stopped by the twin interface boundaries from penetrating into neighboring grains.

Acknowledgements

Much of this work was performed in the EPIC facility of the NUANCE Center at Northwestern University. The research was partially supported by US DOE Grant DE-FG02-02ER46002 at Northwestern University and contract DE-AC52-07NA27344 at Lawrence Livermore National Laboratory.

References

- [1] E.O. Hall, Proc. R. Soc. Lond. B 64 (1951) 474.
- [2] N.J. Petch, J. Iron Steel Inst. 174 (1953) 25.
- [3] K.S. Kumar, H. Van Swygenhoven, S. Suresh, Acta Mater. 51 (2003) 5743.
- [4] L. Lu, Y. Shen, X. Chen, L. Qian, K. Lu, Science 304 (2004) 422.
- [5] K. Zhang, J.R. Weertman, J.A. Eastman, J. Appl. Phys. Lett. 87 (2005) 061921.
- [6] M. Dao, L. Lu, Y.F. Shen, S. Suresh, Acta Mater. 54 (2006) 5421.
- [7] X. Zhang, H. Wang, X.H. Chen, L.Lu.K. Lu, R.G. Hoagland, A. Misra, App. Phys. Lett. 88 (2006).
- [8] O. Anderoglu, A. Misra, H. Wang, F. Ronning, M.F. Hundley, X. Zhang, Appl. Phys. Lett. 93 (2008) 083108.
- [9] O. Anderoglu, A. Misra, H. Wang, X. Zhang, J. Appl. Phys. 103 (2008) 094322.
- [10] A.M. Hodge, Y.M. Wang, T.W. Barbee Jr., Mater. Sci. Eng. A 429 (2006) 272.
- [11] A.M. Hodge, Y.M. Wang, T.W. Barbee Jr., Scripta Mater. 59 (2008) 163.
- [12] K. Zhang, J.R. Weertman, unpublished data.
- [13] E. Ma, Y.M. Wang, Q.H. Lu, M.L. Sui, L. Lu, K. Lu, Appl. Phys. Lett. 85 (2004) 4932.
- [14] L. Lu, R. Schwaiger, Z.W. Shan, M. Dao, K. Lu, S. Suresh, Acta Mater. 53 (2005) 2169.
- [15] T. Zhu, J. Li, A. Samanta, H.G. Kim, S. Suresh, Proc. Natl. Acad. Sci. 104 (2007) 3031.
- [16] H.W. Höppel, M. Kautz, C. Xu, M. Murashkin, T.G. Langdon, R.Z. Valiev, H. Mughrabi, Int. J. Fat. 28 (2006) 1001.
- [17] P.L. Gai, K. Zhang, J.R. Weertman, Scripta Mater. 56 (2007) 25.